Electronic Supplementary Material (ESI) for Physical Chemistry Chemical Physics.

Electronic Supplementary Information

Combined Effects of Emitter-Emitter and Emitter-Plasmonic Surface Separations Dictate Photoluminescence Enhancement in Plasmonic Field

Elizabeth Mariam Thomas,[a] Cristian L. Cortes,[b] Livin Paul,[a] Stephen K. Gray,[b] K. George Thomas[a]**

[a]School of Chemistry, Indian Institute of Science Education and Research Thiruvananthapuram (IISER TVM), Vithura, Thiruvananthapuram, 695 551, India.

[b]Center for Nanoscale Materials, Argonne National Laboratory, Argonne, Illinois 60439, United States.

1. Materials

The following chemicals, cadmium oxide (CdO), trioctylphosphine (TOP), trioctylphosphine oxide (TOPO), selenium powder (Se), zinc acetate, oleic acid, octadecene, oleylamine, trioctylamine, L-cysteine, gold(III) chloride trihydrate, trisodium citrate dihydate, poly(allylamine hydrochloride) (average mw = 17,500) are purchased from Sigma Aldrich. Sodium chloride and potassium hydroxide are purchased from Merck and tetradecylphosphonic acid (TDPA) is purchased from Alfa Aesar. HPLC grade hexane, methanol, isopropanol and acetone are purchased from Spectrochem.

2. Characterization of CdSe/ZnS

CdSe/ZnS is characterized using transmission electron microscopy and found that they are monodisperse and highly crystalline (Fig. S1). The first excitonic peak of CdSe/ZnS in the absorption spectra, corresponding to the band edge transition, is observed at 551 nm. (Fig. S1) The emission spectra showed a maximum at 561 nm. The core size of nanoparticle is found using the empirical relation given by Mulvaney and co-workers[1] and found to be 3.26 nm. All the

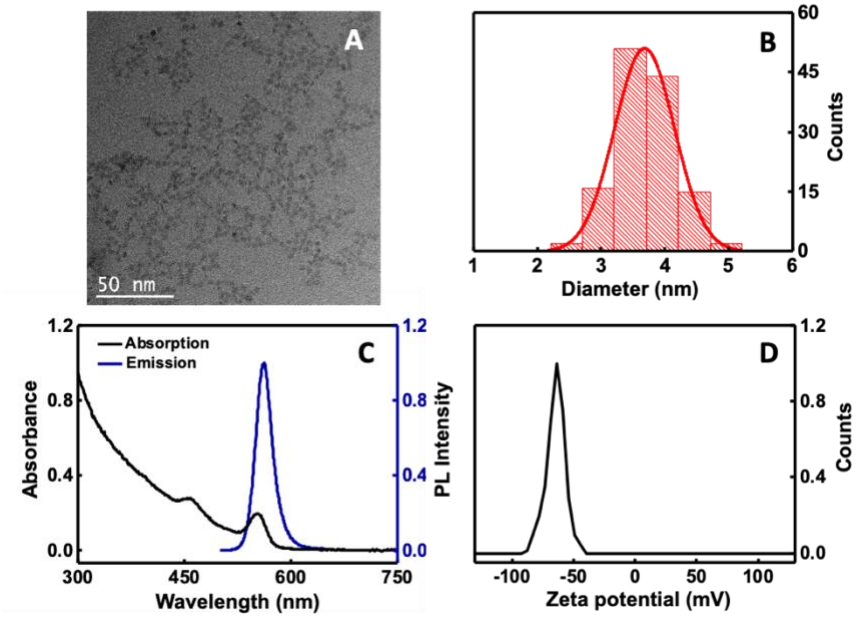

Fig. S1 (A) TEM image, (B) size histogram, (C) absorption and emission spectra and (D) zeta potential distribution of CdSe/ZnS capped with L-cysteine. Note: For steady state PL experiments, CdSe/ZnS are excited at 375 nm keeping excitation and emission slit width as 2 nm.

photophysical studies are carried out in double-distilled water. PL quantum yield of CdSe/ZnS in water is estimated as 2.1 x 10^{-3} by adopting a relative method using Coumarin 153 in ethanol as the reference. Both sample and reference are excited at 375 nm, keeping their optical density (0.075) matched. The surface charge of L-cysteine capped CdSe/ZnS is found to be negative with a zeta-potential (ζ-potential) value of –60.0 mV.

3. Characterization of plasmonic nanoparticles

The nanoparticles formed are characterized using TEM imaging, UV-vis-absorption spectroscopic and ζ-potential studies. The TEM image shows that the formed Au nanoparticles (AuNPs) are monodisperse and a diameter of ~33 nm is obtained. The extinction maximum of AuNPs at 535 nm exhibited a red shift upon silica coating. (Fig. S2) The coating of PAH is confirmed by ζ-potential measurements. The thickness of the spacer (PAH as well as silica having a coating of PAH) are estimated using TEM measurements. Silica coated Au nanoparticle having a layer of PAH is abbreviated as Au-SiO_2 with thickness indicated in parenthesis. Au nanoparticle having a layer of PAH is abbreviated as Au with thickness indicated in parenthesis. The ζ-potential values

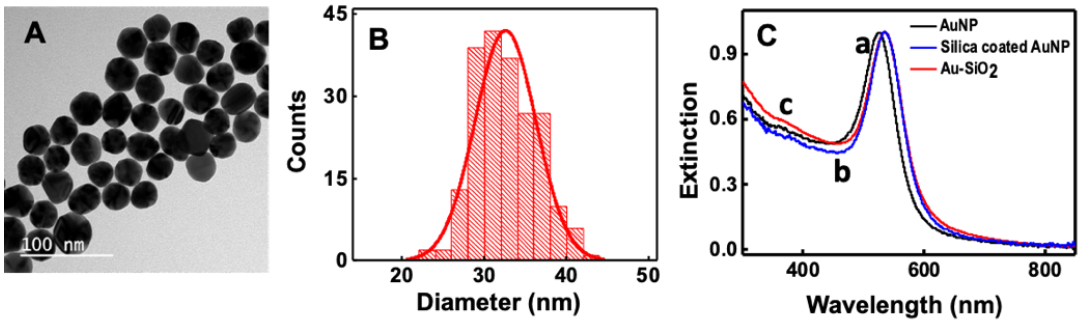

Fig. S2 (A) The TEM image and (B) histogram of AuNPs having diameter of ~33 nm. (C) The extinction spectra of Au nanoparticles at various stages of coating with SiO_2 and PAH: (a) AuNP, (b) overcoated with SiO_2 and (c) further with PAH. The final thickness of the spacer is ~17.3 nm. Note: Silica coated Au nanoparticle having a layer of PAH is abbreviated as Au-SiO_2. Histogram is plotted by measuring the spacer thickness of around 100 particles.

for Au(1.35), Au-SiO_2(5.6), Au-SiO_2(10.8) and Au-SiO_2(17.3) are estimated as +57.1 mV, +51.9 mV, +54.3 mV and +58.7 mV, respectively. The extinction spectra remain unaffected on coating with PAH. Extinction spectra of AuNP, silica coated gold nanoparticle and Au-SiO_2(17.3) are presented in Fig. S2C.

4. Characterization of SiO_2 NPs

TEM image and histogram show that the formed silica nanoparticles (SiO_2 NPs) are spherical having an average diameter of 162 nm (Fig. S3A-C). Extinction spectra displayed in Figure S3D does not possess any well-defined peak, which is a characteristic feature of silica nanoparticles. The concentration of silica nanoparticles is found using inductively coupled plasma-optical emission spectroscopy (ICP-OES). Details are presented in Section 6(iii) of the ESI.

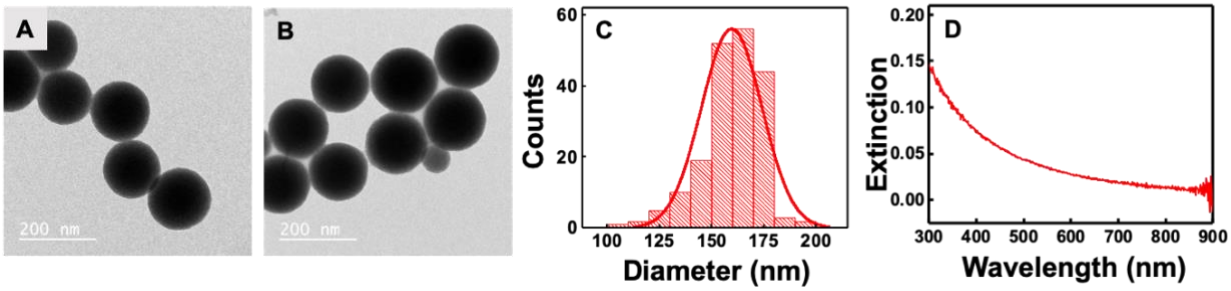

Fig. S3 (A, B) TEM images and (C) histogram of SiO_2 NPs having diameter of ~162 nm. (D) The extinction spectrum of SiO_2 NP. Note: Histogram is plotted by measuring the diameter of around 100 SiO_2 NPs.

5. Calculations of number of QDs/nanoparticle

Probing the PL of CdSe/ZnS by tuning the centre-to-centre distance (s) between the QDs when bound on the surface of plasmonic nanoparticle having various spacer thickness (t) is one of the main objectives of the investigation. The surface area (SA) of plasmonic as well as silica nanoparticles is first estimated and divided into square cells with the objective of placing one CdSe/ZnS at the centre of each cell as presented in Scheme S1. The ‘s’ values are tuned by changing the dimension of the cell. Thus, the maximum number of CdSe/ZnS that can be placed on a given plasmonic/silica nanoparticle is obtained by dividing SA with the area of the square cell.

Scheme S1: Illustration of CdSe/ZnS occupied in a square cell having length 's'[a]

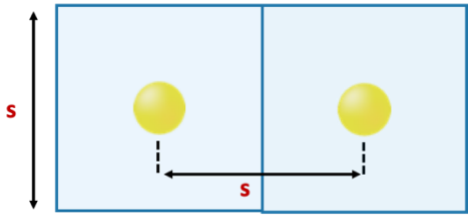

[a]'s' denotes QD-QD separations, i.e., the center-to-center distance between the adjacent QDs (yellow spheres) on the surface of the nanoparticle (blue tiles).

Surface area of a plasmonic/silica nanoparticle (SA) = $4\pi r^2$
(where 'r' is the radius of the nanoparticle)

Area of the square cell containing CdSe/ZnS (a) = s^2
(where 's' is the side of the square cell as well as centre-to-centre distance of CdSe/ZnS)

No. of CdSe/ZnS per nanoparticle = SA/a

The concentration of plasmonic nanoparticle is made constant as 310 pM for all the studies.

Conc. of CdSe/ZnS for 310 pM of plasmonic nanoparticles = 310 SA/a pM

SiO_2 NPs are used as a platform for binding QDs to a surface where the effect of electric field is absent. Similar calculations are done to obtain the number of QDs per SiO_2 NP. Concentration of SiO_2 NPs used for studies is 32 pM. From the SA of SiO_2 NP (radius ~80.5 nm; SA = 8.14 x 10^4 nm^2), the number of CdSe/ZnS per nanoparticle is estimated.

Conc. of CdSe/ZnS for 32 pM of SiO_2 NPs = 32 SA/a pM

The maximum number of QDs that can be placed on the surface of a plasmonic/silica nanoparticles at various QD-QD separations (centre-to-centre) is given in Table S1.

Table S1. No. of QDs per nanoparticle for various separation (s) and spacer thickness (t)

Separation (nm)	No. of QDs/Nanoparticle				
	Au(1.35)	Au-SiO_2(5.6)	Au-SiO_2(10.8)	Au-SiO_2(17.3)	SiO_2 NP
8	59	90	137	210	1193
13	23	35	53	82	463
18	12	18	28	43	244

6. Concentration of nanoparticles

Concentration of various nanoparticles are estimated using analytical/spectroscopic methods.

(i) Au nanoparticles

The extinction coefficient (ε_{max}) of gold nanoparticle at the plasmon band maxima is estimated using the power law expression which relates ε_{max} to its diameter (d).[2]

The power law is given as

$$\varepsilon_{max} = A\left(d/_{nm}\right)^{\gamma}, \quad \text{S1}$$

where A = 4.7 × 10^4 $M^{-1}cm^{-1}$ and γ = 3.30 are constants. The 'd' of Au nanoparticle is obtained from TEM measurements (~33 nm). ε_{max} of Au nanoparticle is estimated as 4.82 x 10^9 $M^{-1}cm^{-1}$ and the concentration of particles are deduced using the Beer-Lambert law. The concentration of plasmonic nanoparticles used to investigate the effect of PL of QDs is kept constant as 310 pM.

(ii) CdSe/ZnS

The extinction coefficient at the first excitonic peak and the concentration of QDs are estimated using the eqns (S2) and (S3), respectively as given by Mulvaney and co-workers.[1]

The extinction coefficient (ε_{1S}) at the first excitonic peak is estimated using the eqn (S2),

$$\varepsilon_{1S} = 155507 + 6.67054 \times 10^{13}\, e^{\left(-E_{1S}/_{0.10551}\right)} \quad \text{S2}$$

$where, E_{1S}$ is the energy in eV at its first excitonic peak.

The concentration of CdSe/ZnS is calculated using the Beer-Lambert law with slight modification, eqn (S3).[1] The modification in the equation is to account for the size distribution. Concentration (C) of CdSe/ZnS is given as,

$$C = \frac{Abs}{l \times \varepsilon_{1S}} \times \frac{\Delta E_{1S,HWHM}}{0.06} \qquad \text{S3}$$

where, l is the path length of the cuvette in cm, Abs is the absorption at the first excitonic peak and $\Delta E_{1S,HWHM}$ is the half-width at half-maximum of first excitonic peak in eV.

(iii) SiO_2 nanoparticles

Concentration of SiO_2 NP is found out using ICP-OES and TEM analysis.

Concentration of SiO_2 is estimated as 778.6 ppm (778.6 mg/L) in 5 mL from ICP-OES analysis.

Mass of SiO_2 in 5 mL = 778.6 mg/L x 5 mL = 3.89 mg

Diameter (d) of the particle obtained from TEM is 161 nm

Volume of a SiO_2 NP $= \frac{4}{3}\pi\left(\frac{d}{2}\right)^3$

$= \frac{4}{3}\pi(80.5\ nm)^3 = 2.18 \times 10^6\ nm^3$

Density of SiO_2 NP $= 2.0\ gcm^{-3}$

Mass of one SiO_2 NP $= 2.0\ gcm^{-3} \times 2.18 \times 10^6\ nm^3 = 4.36 \times 10^{-15}\ g$

No. of SiO_2 NP in 5 mL = mass of SiO_2/mass of one SiO_2 NP

$= 3.89\ mg / 4.36 \times 10^{-15}\ g = 0.892 \times 10^{12}$

No. of moles of SiO_2 NP in 5 mL $= 0.892 \times 10^{12} / 6.023 \times 10^{23} = 0.148 \times 10^{-11}\ mol$

Molar concentration of SiO_2 NP $= 0.148 \times 10^{-11}\ mol / 5\ mL = 0.29\ nM$

7. Preparation of QD-plasmonic hybrids

7.1. Extinction spectrum of CdSe/ZnS bound on plasmonic/silica nanoparticles

The extinction spectra of the CdSe/ZnS bound to Au(1.35), Au-SiO_2(5.6), Au-SiO_2(10.8) and Au-SiO_2(17.3) at different s values, overlaps with the extinction spectra of its respective plasmonic nanoparticles (Fig. S4) ruling out the possibility of any aggregation.

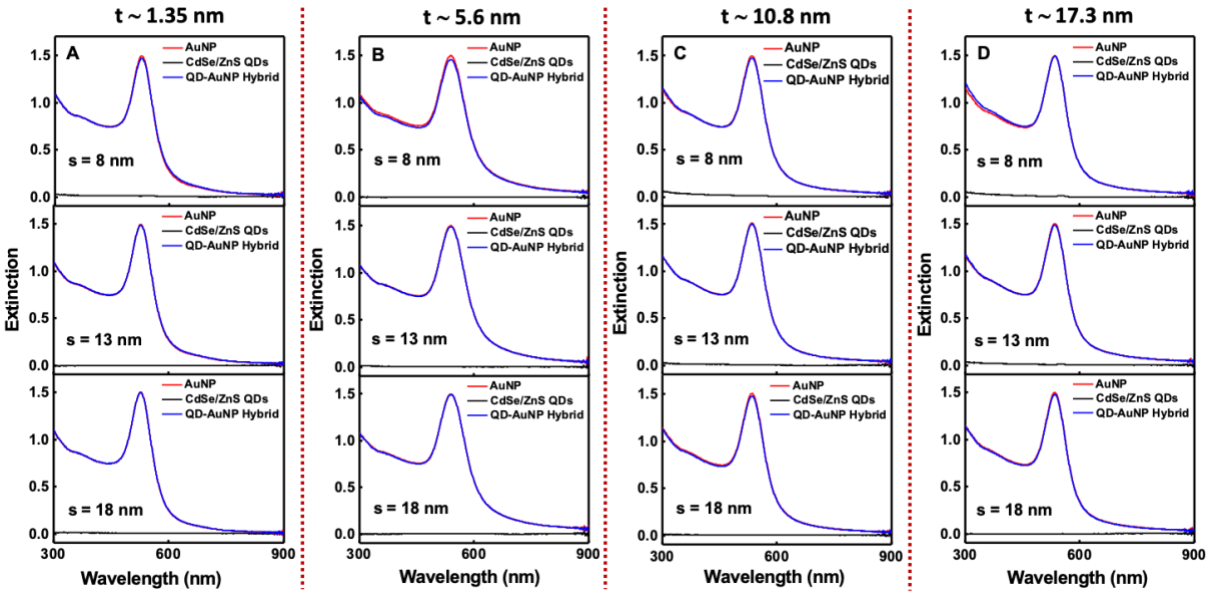

Fig. S4 Extinction spectra of (A) Au(1.35) (B) Au-SiO_2(5.6), (C) Au-SiO_2(10.8) and (D) Au-SiO_2(17.3) in the absence (red trace) and presence (blue trace) of CdSe/ZnS at different separation s = 8 nm (top panel), s = 13 nm (middle panel) and s = 18 nm (bottom panel).

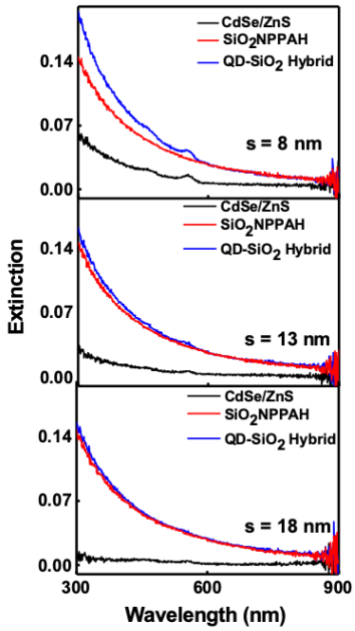

Fig. S5 Extinction spectra of SiO_2 NPs in the absence (red trace) and presence (blue trace) of CdSe/ZnS at different separation s = 8 nm (top panel), s = 13 nm (middle panel) and s = 18 nm (bottom panel). Absorption spectra of CdSe/ZnS used in each case are given as black traces.

7.2. Stability of CdSe/ZnS bound on plasmonic nanoparticles

QD bound plasmonic hybrid systems in water (3 mL) are constructed by adding required concentration of CdSe/ZnS having negative surface charge to plasmonic systems having positive surface charge. Experiments are carried out in a quartz cuvette having a path length of 1 cm. The hybrid solution is then equilibrated for 10 min before the measurement.

The extinction spectra of the CdSe/ZnS bound on Au(1.35), measured as a function of time, remained same indicating that the hybrid system is stable (Fig S6A). Optical density at the extinction maximum (528 nm) and half-width at half-maximum (HWHM), plotted as a function of time (Fig. S6B,C), remained constant. These results indicate that there is no decrease in extinction or broadening of spectra for the hybrid systems with time which demonstrates the colloidal stability of hybrid system.

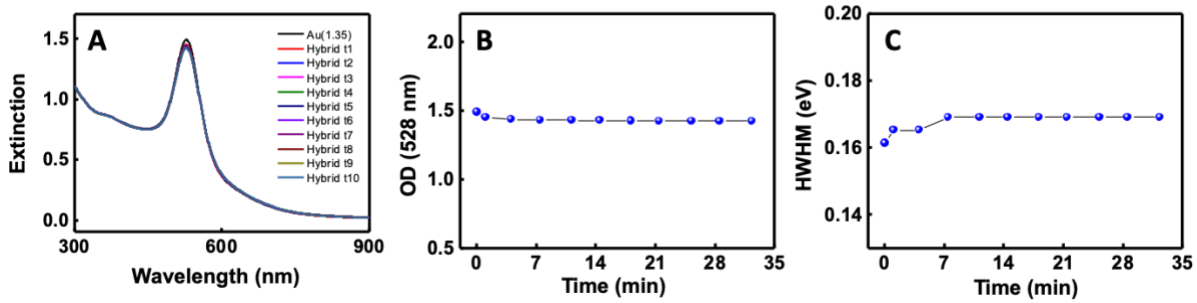

Fig. S6 Extinction spectra of hybrids of CdSe/ZnS bound on Au(1.35) at s = 8 nm measured as a function of time. (A) Traces t1 - t10 represent various spectrum recorded, at a time interval of 3 min, up to 30 min. (B) Optical density of the hybrid systems at 528 nm and the (C) corresponding half-width half-maxima plotted against time, obtained from (A).

7.3. Zeta potential and number density of CdSe/ZnS bound on plasmonic nanoparticles

Zeta potentials of the solution are monitored before and after addition of CdSe/ZnS to confirm the binding of negatively charged QDs on positively charged plasmonic nanoparticles. The zeta potentials of the solution remained highly positive even at the highest number density of QDs (Figure S7) ruling out the possibility unbound CdSe/ZnS in solution.

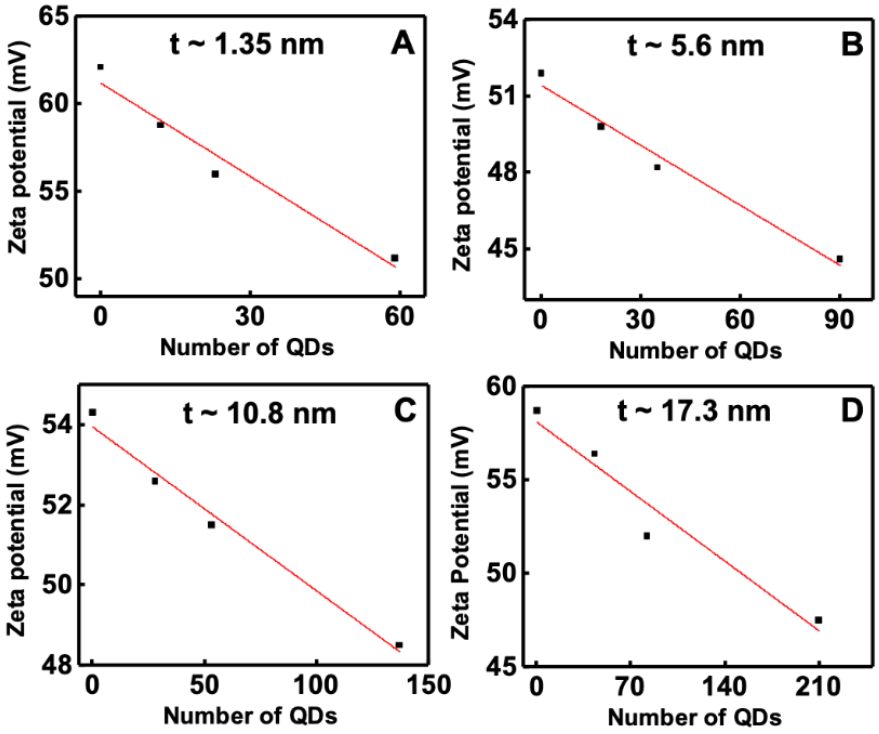

Fig. S7 Zeta potential of CdSe/ZnS bound on (A) Au(1.35), (B) Au-SiO_2(5.6), (C) Au-SiO_2(10.8), and (D) Au-SiO_2(17.3) as a function of number of QDs. Number of QDs required to obtain a separation of 8, 13 and 18 nm are estimated in each case (see, Table S1).

7.4. Centrifugation of CdSe/ZnS bound on plasmonic nanoparticles

Attempts are made to quantify the number of QDs that are electrostatically bound on Au-SiO_2/SiO_2 surface. We have centrifuged CdSe/ZnS bound on Au(1.35) (s = 8 and 18 nm) at 6000 rpm for 20 min and collected the residue and supernatant. The extinction spectrum of the supernatant showed contributions from both Au(1.35) and CdSe/ZnS. The extinction features of supernatant (pink trace in Fig. S8B) for s = 8 nm at the lower wavelength range (below 500 nm) are similar to those of CdSe/ZnS indicating greater contribution from the absorbance of QDs. This is further verified by estimating the ratio of extinction at 528 nm (extinction maximum of AuNP) and 375 nm, a wavelength wherein the absorbance of QD is high. The ratio is found to be 1.73 for CdSe/ZnS bound on Au(1.35) (s = 8 nm) which reduced to 0.94 for the supernatant and 1.68 for residue (volume kept at 3 mL). The decreased ratio of extinction for the supernatant is due to the presence of large excess of QDs in the solution. Upon centrifugation, CdSe/ZnS which are electrostatically bound on Au(1.35) tend to detach and stay in the supernatant while Au nanoparticles settle down.

A similar observation is obtained for s = 18 nm. Attempts made to separate the unbound CdSe/ZnS, if any, by varying the centrifugation speed and time are also not successful.

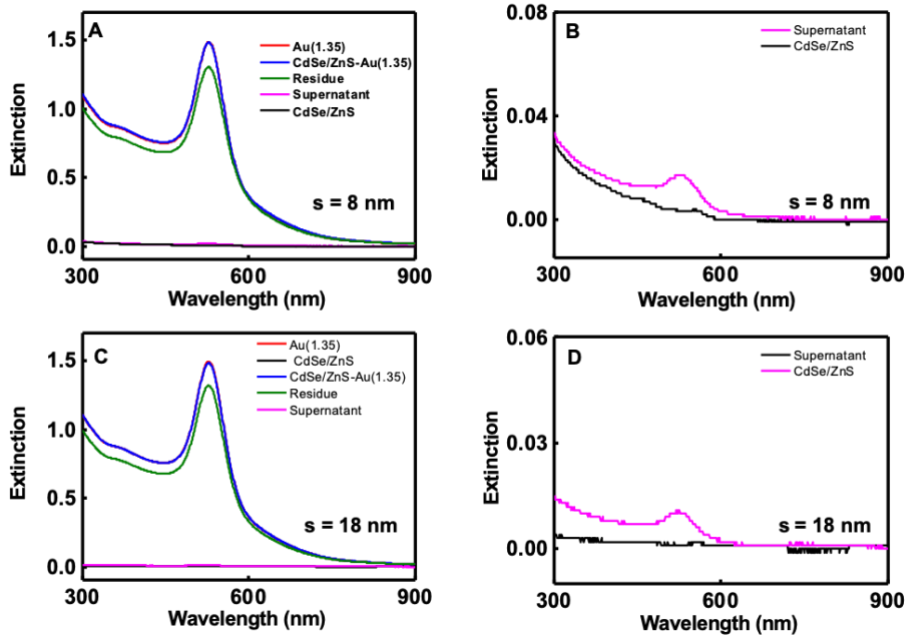

Fig. S8 (A,C) Extinction spectra of Au(1.35) (red trace), CdSe/ZnS (black trace; see B and D for clarity), CdSe/ZnS bound on Au(1.35) (blue trace), residue (green trace) and supernatant solution (pink trace) obtained after centrifugation at 6000 rpm for 20 min having a separation of s = 8 nm (A) and s = 18 nm (C). (B,D) The extinction spectra (enlarged) of supernatant and CdSe/ZnS for s = 8 nm (B) and s = 18 nm (D) are provided for clarity: CdSe/ZnS (black trace), supernatant solution (pink trace).

8. Correction factors

Two different correction factors are used to account for the primary and secondary inner filter effects (IFE).

CF for IFE - method 1: Correction factor for IFE_{m1} is estimated by monitoring the absorbance of QD-bound plasmonic hybrid at the excitation wavelength (375 nm) and emission wavelength (561 nm) following the method reported by Lakowicz.[3] Correction factor is given as

$$IFE_{m1} = 10^{(A_{ex} + A_{em})/2}, \qquad \text{S4}$$

where A_{ex} and A_{em} represent the absorbance at the excitation wavelength (375 nm) and emission wavelength (561 nm), respectively.

Absorbance is $\log_{10}(I_0/I) = -\log_{10}(T)$ where $T = I/I_0$ is the transmittance, the fraction of light that passes through the sample in the presence of nanoparticles. Equation S4 can then be seen to be simply the geometric average of the product of the inverse transmittances,

$$IFE_{m1} = \left(\frac{1}{T_{ex}}\frac{1}{T_{em}}\right)^{1/2}, \quad \text{S5}$$

where T_{ex} and T_{em} represent the transmittance at the excitation and emission wavelengths, respectively.

CF for IFE - method 2 (cell shift method): The correction factor (method 2) for IFE_{m2} is based on a mathematical model[4] involving effective beam width of excitation (Δy) and emission light (Δx) as

$$IFE_{m2} = \frac{2.303A_{ex}\,\Delta x\, 10^{A_{ex}\,x_1}}{1-10^{-A_{ex}\Delta x}}\,\frac{2.303A_{em}\Delta y\, 10^{A_{em}\,y_1}}{1-10^{-A_{em}\Delta y}}, \quad \text{S6}$$

where x_1 and y_1 are the distances from inner wall of cuvette to the edge of beam in x-direction and y-direction, respectively.

The effective beam width of excitation and emission light is obtained by measuring the PL intensity as a function of the displacement of the cuvette in the beam path following a procedure given by Gu and Kenny.[5] PL measurements are carried out by mounting cuvette (1 cm path length) on a micrometre driven 3D translation stage (Scheme S2). Quinine sulphate in H_2SO_4 (0.1 M) is used as the standard dye and is excited at 345 nm and emission is monitored at peak maxima (450 nm). The excitation and emission slit width is kept at 2 nm as used in QD-plasmon hybrid systems. Beam width Δ*x* is obtained by moving the cuvette towards the excitation source (x-direction) at a step size of 1 mm with y-coordinate fixed at the center of the cuvette. Similar scan is done in y-direction with x-coordinate fixed at the center of cuvette to obtain Δ*y*. The PL intensity is

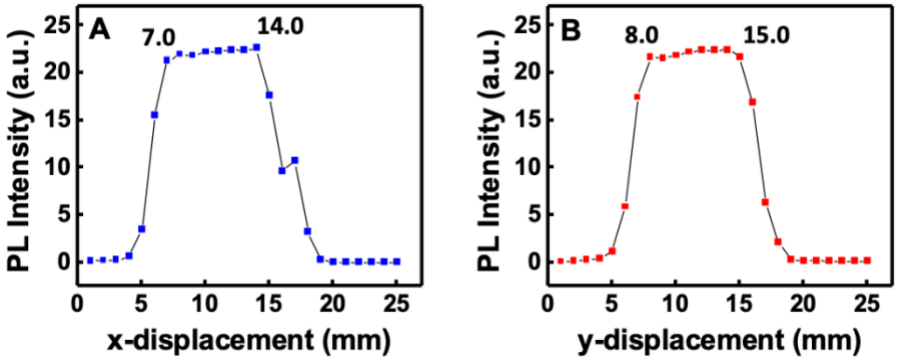

Fig. S9 Plot of PL intensity as a function of displacement along (A) x- and (B) y-directions.

maximum and remains constant when the effective beam is completely inside the cell and afterwards a sharp decline in intensity is observed. The displacement having maximum constant PL intensity (Δ*s*) is estimated as 0.3 mm in both x- and y-directions. The effective beam width is obtained by subtracting Δ*s* from the path length of cuvette.

Scheme S2: Illustration of (A) effective excitation and emission beam passing through the cuvette (B) cell shift in x- and y-directions.[a]

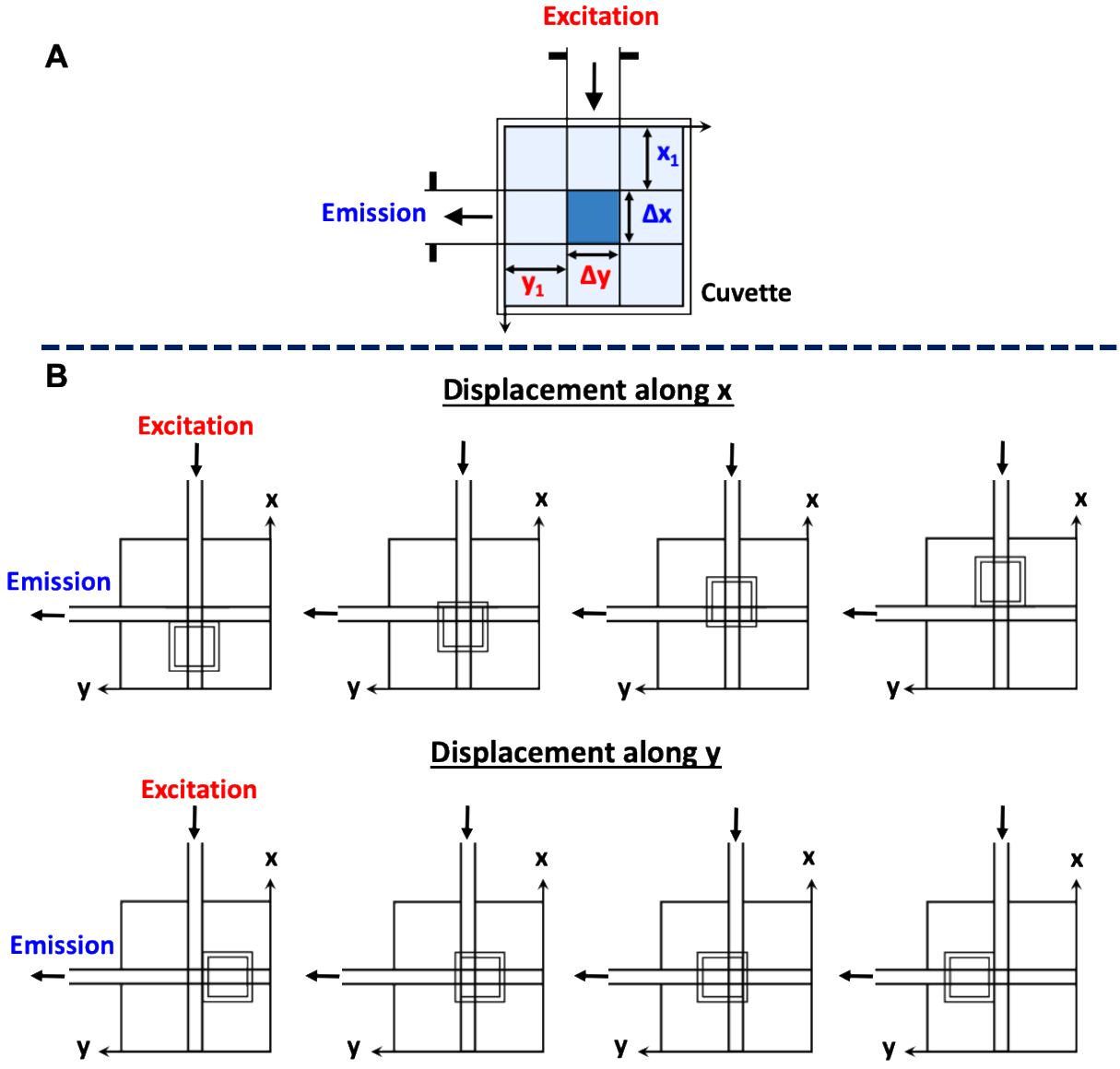

[a]Parallel lines represent the effective excitation and emission beams.

9. Photophysical studies of CdSe/ZnS on plasmonic/silica nanoparticles

Variation of ζ-potential on addition of CdSe/ZnS to plasmonic/silica nanoparticles at different s, experimental enhancement factor obtained before and on applying CF using method 1 and method 2 are tabulated in Tables S2-S6. The thickness of spacer on plasmonic nanoparticles is provided in parenthesis.

9.1. Photophysical studies of CdSe/ZnS on Au(1.35)

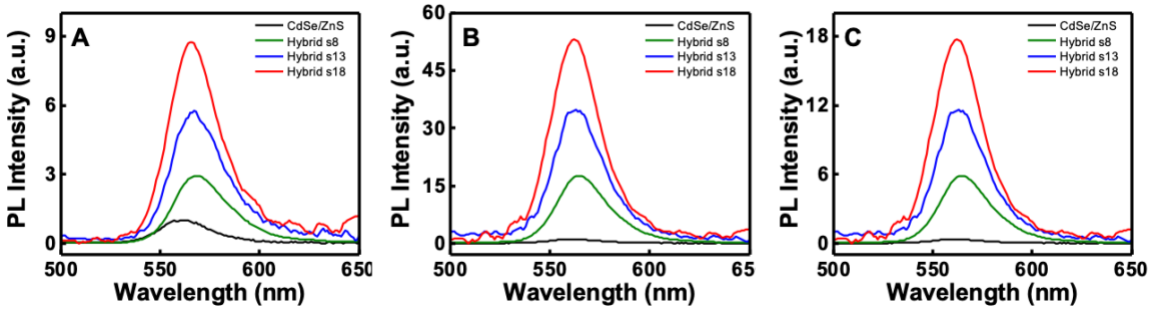

Fig. S10 (A) Uncorrected and (B,C) corrected PL spectra of CdSe/ZnS bound to Au(1.35) by varying the separation (s) between the CdSe/ZnS as 8 (green trace), 13 (blue trace), and 18 nm (red trace). Correction for inner filter effect is applied on the CdSe/ZnS-Au(1.35) hybrid (A) and presented as (B). Further surface effect correction is applied on B and presented as (C).

Table S2. The emission enhancement factor of CdSe/ZnS for various separation on Au(1.35)

Hybrid system	Separation (nm)	No. of QDs/AuNP	Zeta potential (mV)	I_{Obs}/I_0	EF_{exp}	EF_{exp} (cs)
CdSe/ZnS-Au(1.35)	8	59	+ 51.2	2.43	5.54	5.40
CdSe/ZnS-Au(1.35)	13	23	+ 56.0	4.83	10.49	10.22
CdSe/ZnS-Au(1.35)	18	12	+ 58.8	7.67	17.35	16.88
Au(1.35)	-	-	+ 62.1	-	-	

9.2. Photophysical studies of CdSe/ZnS on Au-SiO_2(5.6)

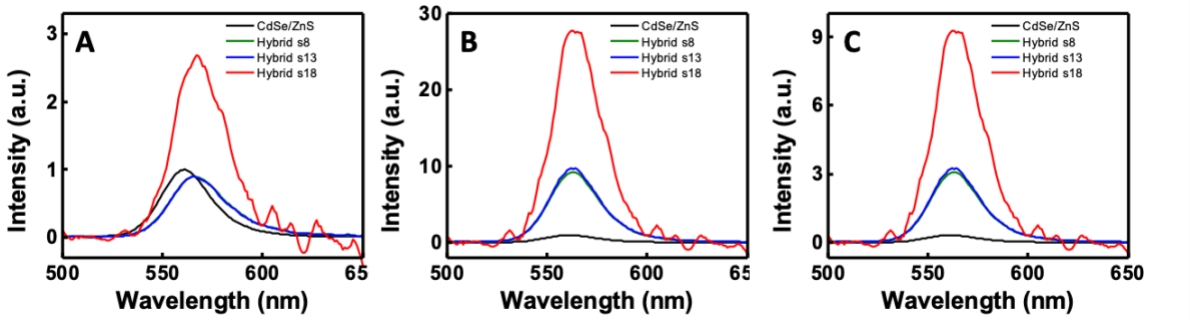

Fig. S11 (A) Uncorrected and (B,C) corrected PL spectra of CdSe/ZnS bound to Au(5.6) by varying the separation (s) between the CdSe/ZnS as 8 (green trace), 13 (blue trace), and 18 (red trace) nm. Correction for inner filter effect is applied on the CdSe/ZnS-Au(5.6) hybrid (A) and presented as (B). Further surface effect correction is applied on B and presented as (C).

Table S3. The emission enhancement factor of CdSe/ZnS for various separation on Au-SiO_2(5.6)

Hybrid system	Separation (nm)	No. of QDs/AuNP	Zeta potential (mV)	I_{Obs}/I_0	EF_{exp}	EF_{exp} (cs)
CdSe/ZnS-Au-SiO_2(5.6)	8	90	+ 44.6	0.821	3.09	2.95
CdSe/ZnS-Au-SiO_2(5.6)	13	35	+ 48.2	0.849	3.28	3.13
CdSe/ZnS-Au-SiO_2(5.6)	18	18	+ 49.8	2.38	9.26	8.83
Au-SiO_2(5.6)	-	-	+ 51.9	-	-	-

9.3. Photophysical studies of CdSe/ZnS on Au-SiO_2(10.8)

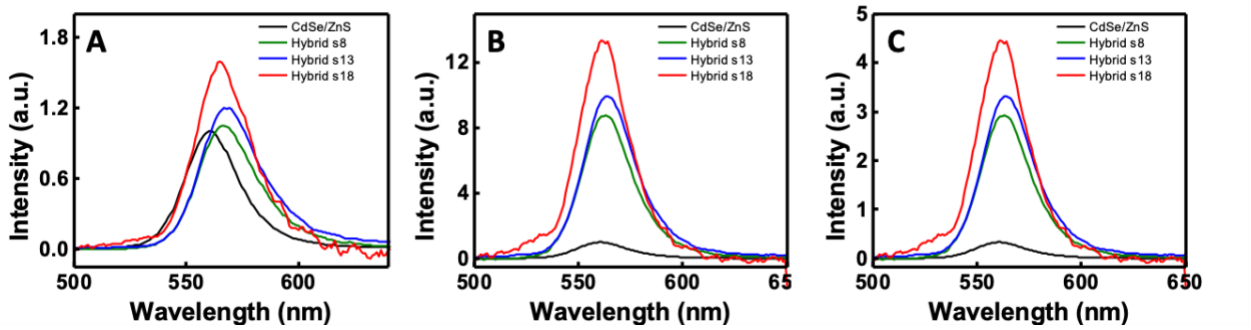

Fig. S12 (A) Uncorrected and (B,C) corrected PL spectra of CdSe/ZnS bound to Au(10.8) by varying the separation (s) between the CdSe/ZnS as 8 (green trace), 13 (blue trace), and 18 (red trace) nm. Correction for inner filter effect is applied on the CdSe/ZnS-Au(10.8) hybrid (A) and presented as (B). Further surface effect correction is applied on B and presented as (C).

Table S4. The emission enhancement factor of CdSe/ZnS for various separation on Au-SiO_2(10.8)

Hybrid system	Separation (nm)	No. of QDs/AuNP	Zeta potential (mV)	I_{Obs}/I_0	EF_{exp}	EF_{exp} (cs)
CdSe/ZnS-Au-SiO_2(10.8)	8	137	+ 48.5	0.93	2.89	2.78
CdSe/ZnS-Au-SiO_2(10.8)	13	53	+ 51.5	1.00	3.14	3.02
CdSe/ZnS-Au-SiO_2(10.8)	18	28	+ 52.6	1.92	5.86	5.63
Au-SiO_2(10.8)	-	-	+ 54.3	-	-	-

9.4. Photophysical studies of CdSe/ZnS on Au-SiO_2(17.3)

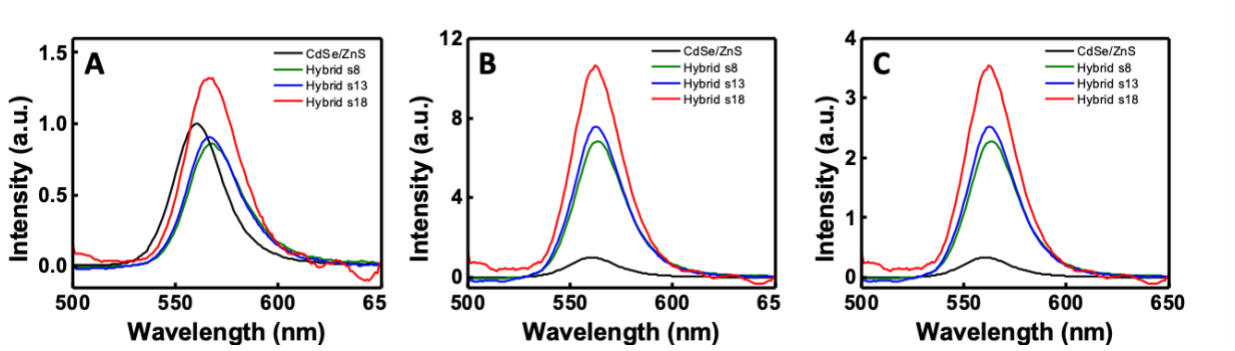

Fig. S13 (A) Uncorrected and (B,C) corrected PL spectra of CdSe/ZnS bound to Au(17.3) by varying the separation (s) between the CdSe/ZnS as 8 (green trace), 13 (blue trace), and 18 (red trace) nm. Correction for inner filter effect is applied on the CdSe/ZnS-Au(17.3) hybrid (A) and presented as (B). Further surface effect correction is applied on B and presented as (C).

Table S5. The emission enhancement factor of CdSe/ZnS for various separation on Au-SiO_2(17.3)

Hybrid system	Separation (nm)	No. of QDs/AuNP	Zeta potential (mV)	I_{Obs}/I_0	EF_{exp}	EF_{exp} (cs)
CdSe/ZnS-Au-SiO_2(17.3)	8	210	+ 47.5	0.73	2.31	2.20
CdSe/ZnS-Au-SiO_2(17.3)	13	82	+ 52.0	0.81	2.50	2.40
CdSe/ZnS-Au-SiO_2(17.3)	18	43	+ 56.4	1.31	3.86	3.70
Au-SiO_2(17.3)	-	-	+ 58.7	-	-	-

9.5. Photophysical studies of CdSe/ZnS on SiO_2 NP

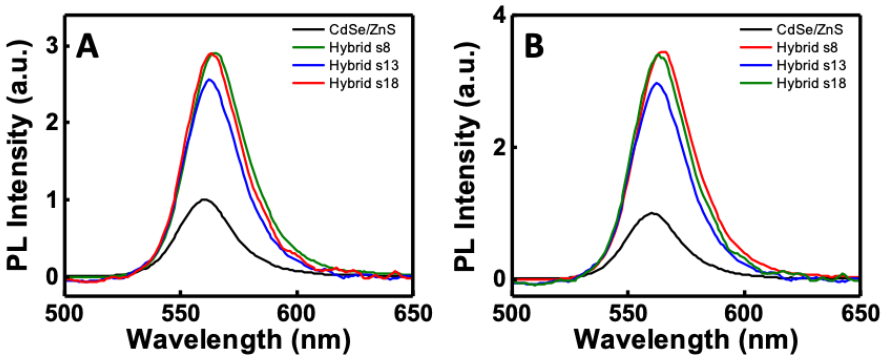

Fig. S14 (A) Uncorrected and (B) corrected PL spectra of CdSe/ZnS bound to SiO_2 NP by applying inner filter effect corrections at various separation (s) between the CdSe/ZnS as 8 (red trace), 13 (blue trace), and 18 nm (green trace).

Table S6. The emission enhancement factor of CdSe/ZnS for various separation on SiO_2 NP

Hybrid system	Separation (nm)	No. of QDs/SiO_2 NP	Zeta potential (mV)	I_{Obs}/I_0	EF_{exp}	EF_{exp} (cs)
CdSe/ZnS-SiO_2 NP	8	1193	+ 31.4	2.74	3.26	3.26
CdSe/ZnS-SiO_2 NP	13	463	+ 35.4	2.51	2.91	2.91
CdSe/ZnS-SiO_2 NP	18	244	+ 43.5	2.57	2.97	2.97
SiO_2 NP	-		+ 47.5	-	-	-

10. Landscape of PL enhancement of CdSe/ZnS using cell shift method

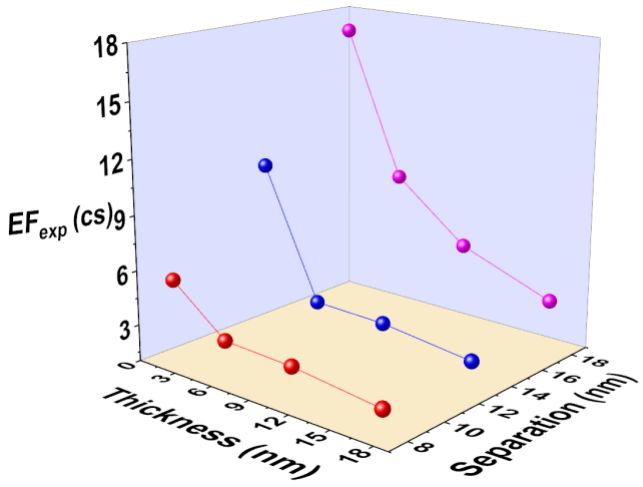

Fig. S15 3D-plot illustrating the enhancement of emission ($EF_{exp}(cs)$) of CdSe/ZnS by varying the spacer thickness (t) and QD-QD separation (s). Note: The experimental enhancement factor obtained by method 2 (cell shift method) is denoted as $EF_{exp}(cs)$. 3D-plot illustrating the enhancement of emission (EF_{exp}) of CdSe/ZnS by varying t and s is presented as Figure 4.

11. PL lifetime of CdSe/ZnS on plasmonic/silica nanoparticles

Table S7. Intensity weighted average lifetimes (τ_{avg})[a] of CdSe/ZnS QDs bound on plasmonic and silica nanoparticles.

CdSe/ZnS on plasmonic/silica NPs	Average lifetimes (τ_{avg}), ns		
	s 18	s 13	s 8
QD on SiO_2NP	0.97	0.98	1.07
QD on Au(1.35)	0.61	0.73	1.01
QD on Au-SiO_2(5.6)	0.48	0.54	1.21
QD on Au-SiO_2(10.8)	0.64	0.84	1.56
QD on Au-SiO_2(17.3)	0.63	0.97	1.44

[a]Intensity weighted average lifetimes (τ_{avg}) are calculated after excluding the long lifetime component since its contribution is less than 2%, in all the cases.

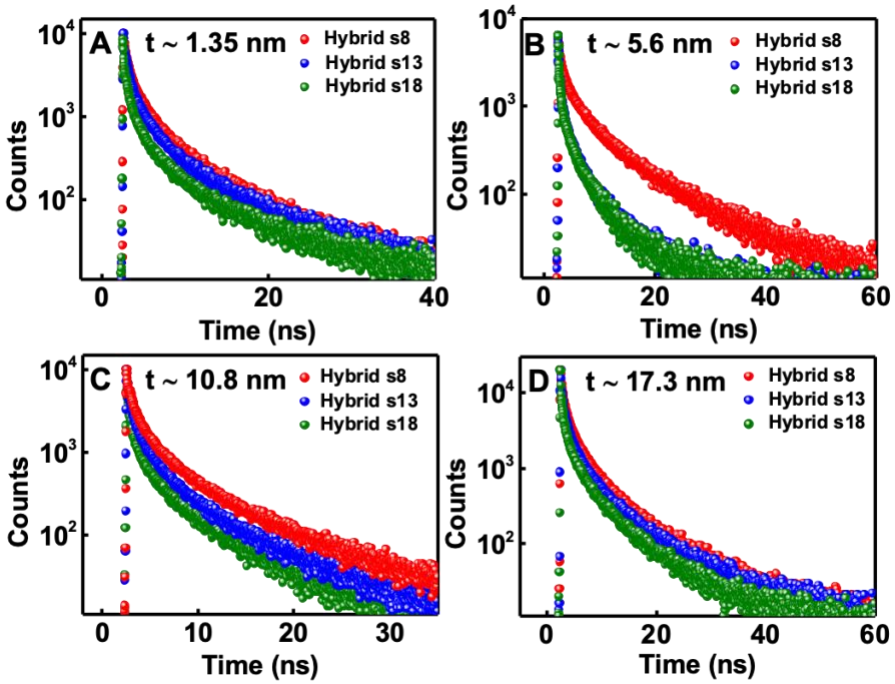

Fig. S16 The PL decay of CdSe/ZnS bound on (A) Au(1.35), (B) Au-SiO_2(5.6), (C) Au-SiO_2(10.8), and (D) Au-SiO_2(17.3) with separation s = 8 (red spheres), 13 (blue spheres) and 18 nm (green spheres).

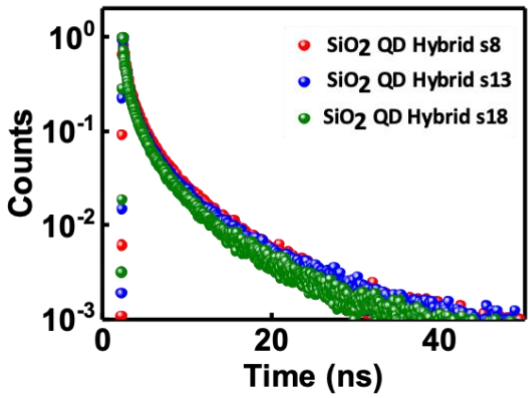

Fig. S17 The PL decay of CdSe/ZnS bound on SiO_2 NP with separation s = 8 (red spheres), 13 (blue spheres) and 18 nm (green spheres).

12. Model system and theoretical methods

We take, as a base system, a spherical AuNP of diameter d_{Au} = 33 nm described by the Johnson and Christy frequency-dependent and complex refractive index.[6] We assume the medium around this NP is water (refractive index 1.33), i.e., for simplicity we consider the silica shell of thickness

t around the AuNP has the same refractive index as water, although it is likely slightly larger. On top of this hypothetical silica surface we then have N quantum dot emitters (QDs), each taken to be a point dipole and placed at a radius (relative to the center of the AuNP) of $R_{QD} = d_{Au}/2 + t + d_{QD}/2$, where d_{QD} is the experimental diameter of the emitters (d_{QD} = 3.8 nm for our CdSe/ZnS). Figure 5A compares theoretical and experimental extinction spectra for isolated AuNPs (d_{Au} = 33 nm) in water, showing excellent overall agreement in terms of spectral features.

For the placement of the N dipole emitters we use numerical solutions to the Thomson problem.[7] The Thomson problem is to find the lowest energy configuration of a system of N particles on a sphere with interaction energy $V = \sum_{i<j} 1/r_{ij}$, where r_{ij} is the distance between particles *i* and *j* and the sum is over all pair-wise interactions. We use a simulated annealing procedure to find the positions of the particles that minimize the interaction energy. As an aside, we note that for N greater than about 70, numerical determination of the absolute minima for the Thomson problem can be quite challenging and sophisticated approaches are required.[7]

The orientations of the point dipole vectors relative to the nanoparticle surface are also very relevant, but challenging. In some instances we have considered the traditional perpendicular and parallel orientations relative to the nanoparticle surface. It is likely, though, that the experiments correspond to some degree of randomization of the dipole orientations. For the case N = 1, a simple orientational average can be carried out by taking one third of the sum of the perpendicular and twice the parallel orientation results, and we have found this is a good approximation to a more extensive orientational average. For N much greater than one, however, we have found that the results are so sensitive to dipole orientations that it is computationally challenging to carry out full orientational averaging and we will restrict ourselves to a simplified average corresponding to one third of all the dipoles oriented along each of the x-, y- and z-directions. This is perhaps more reflective of what happens with linear polarization at the initial excitation wavelength, and some degree of randomization is likely to occur prior to emission that we do not account for the reason stated above.

With the QDs/AuNP model system described above, and assuming each of the N point emitters is emitting at a given frequency (or wavelength), we solve Maxwell's or equivalent equations numerically to obtain the steady-state, complex electric and magnetic fields, E(*x*,*y*,*z*) and H(*x*,*y*,*z*) with *x*,*y*,*z* denoting Cartesian space. Regarding the numerical methods, we employ a generalized multiparticle Mie theory or aggregate T-matrix method[8] for which there is an efficient Python

package.[9] Finally, from the solutions of Maxwell's equations for the model systems discussed above we construct the quantities of relevance to fluorescence, including the normalized radiative and nonradiative rates,[10]

$$f_r = \left(\frac{1}{W_0}\right) \iint_{\Sigma_1} S \cdot d\Sigma \tag{S7}$$

$$f_{nr} = \left(-\frac{1}{W_0}\right) \iint_{\Sigma_2} S \cdot d\Sigma \tag{S8}$$

where the closed surface Σ_1 associated with the surface integral in eqn (S7) contains within it both the QDs and AuNP, but the closed surface Σ_2 associated with the surface integral in eqn (S8) contains within it the AuNP but not the QDs (i.e., it is within the shell t). In these equations, the Poynting vector $S = \left(\frac{1}{2}\right) Re(E \times H^*)$ and the normalization factor W_0 is the surface integral over the Poynting vector for the system of N dipoles but with no AuNP present (i.e., radiated power in the absence of the nanoparticle). Thus f_r is the radiative rate enhancement factor and f_{nr} can also be seen to be the normalized AuNP absorption rate due to the emitter sources.[11] These normalized radiative and nonradiative rates are used in the determination of the fluorescence enhancements as discussed in the main text (see eqns (5)-(7) and discussion).

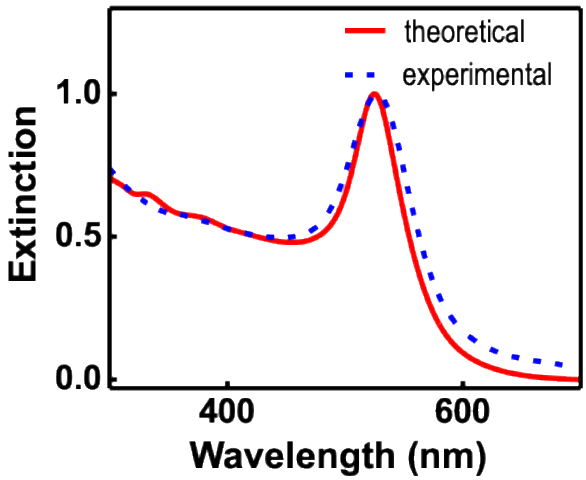

Fig. S18 Theoretical (solid) and experimental (dashed) extinction spectra for a 33 nm diameter Au nanoparticle in water.

13. Theoretical results on increasing the number of QDs

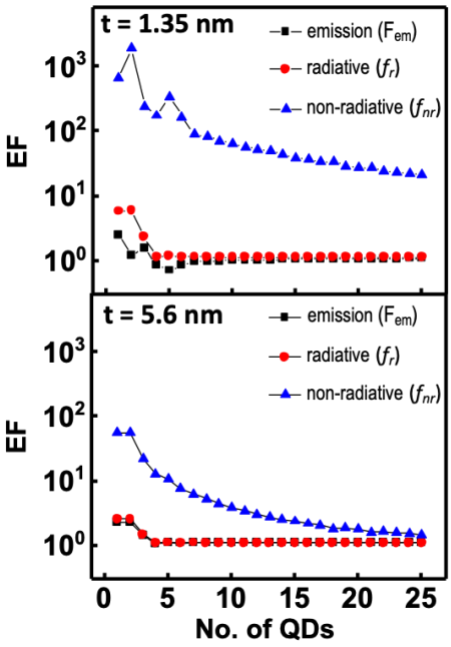

Fig. S19 EF as a function of the number of QDs, N, inferred from our theoretical model, averaging over three polarizations: (top panel) t = 1.35 nm and (bottom panel) t = 5.6 nm.

14. References

1. J. Jasieniak, L. Smith, J. van Embden, P. Mulvaney and M. Califano, *J. Phys. Chem. C*, 2009, **113**, 19468-19474.

2. J. R. G. Navarro and M. H. V. Werts, *Analyst*, 2013, **138**, 583-592.

3. J. R. Lakowicz, *Principles of Fluorescence Spectroscopy*, Springer Academic, New York, 3rd edn., 2006.

4. B. C. MacDonald, S. J. Lvin and H. Patterson, *Anal. Chim. Acta*, 1997, **338**, 155-162.

5. Q. Gu and J. E. Kenny, *Anal. Chem.*, 2009, **81**, 420-426.

6. P. B. Johnson and R.-W. Christy, *Phys. Rev. B*, 1972, **6**, 4370.

7. W. J. M. Ridgway and A. F. Cheviakov, *Comput. Phys. Commun.*, 2018, **233**, 84-109.

8. Y.-l. Xu, *Appl. Opt.*, 1995, **34**, 4573-4588.

9. J. A. Parker, https://github.com/johnaparker/miepy).

10. M. Liu, T.-W. Lee, S. K. Gray, P. Guyot-Sionnest and M. Pelton, *Phys. Rev. Lett.*, 2009, **102**, 107401.

11. C. F. Bohren and D. R. Huffman, *Absorption and Scattering of Light by Small Particles*, John Wiley & Sons, Weinheim, 2008.